PROCEEDINGS

PCF 2014

XIV Portuguese Conference on Fracture

UNIVERSIDADE DE TRÁS-OS-MONTES E ALTO DOURO

utad

PROCEEDINGS

EDITED BY

Abílio de Jesus

Alfredo Ribeiro

José Morais

José Xavier

Nuno Dourado

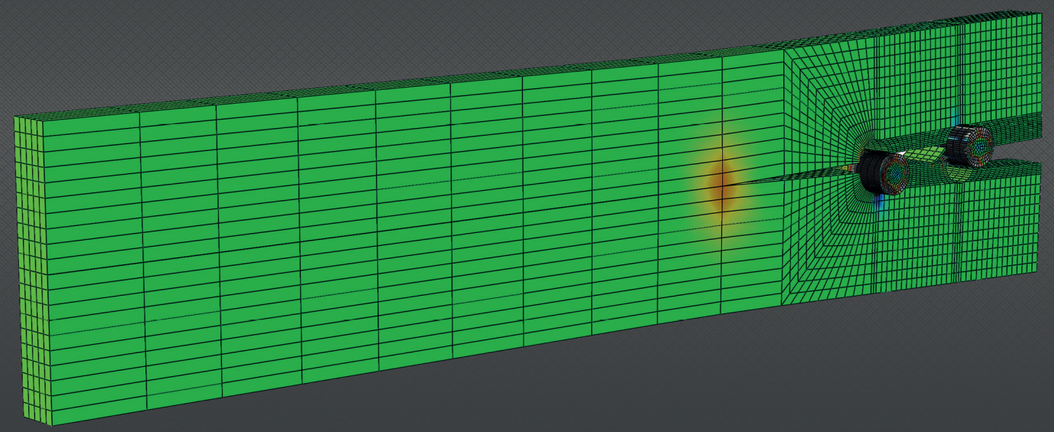

RÉGUA, 6-7TH FEBRUARY, 2014

PCF 2014

XIV Portuguese Conference on Fracture

MIXED-MODE I + II FRACTURE CHARACTERIZATION OF BONDED JOINTS USING A NOVEL MULTI-MODE APPARATUS

Filipe J.P. Chaves [1*], L.F.M da Silva [2], M.F.S.M de Moura [2], D. A. Dillard [3]

[1] IDMEC- Pólo FEUP, Faculdade de Engenharia da Universidade do Porto,
Rua Dr. Roberto Frias, 4200-465 Porto, Portugal.
[2] DEMec, Faculdade de Engenharia da Universidade do Porto,
Rua Dr. Roberto Frias, 4200-465 Porto, Portugal.
[3] Engineering Science and Mechanics Department, Virginia Tech,
Blacksburg, VA 24061

ABSTRACT

The present work presents the experimental test results to assess the toughness of an adhesive joint, using a previously defined crack equivalent data reduction scheme applied to a new multi-mode apparatus, inspired in a load jig previously developed by Fernlund and Spelt. The patented jig allows for easy alteration of the mode-mixity and permits covering the full range of mixed-mode I+II combinations. A data reduction scheme based on specimen compliance, beam theory and crack equivalent concept is used to overcome several difficulties inherent to the test analysis. The method assumes that the performed test can be viewed as a combination of the double cantilever beam and asymmetrically loaded end-notched flexure tests, which provide modes I and II fracture characterization, respectively. A numerical analysis including a cohesive mixed-mode I+II damage model was performed considering different mixed-mode loading conditions to validate the proposed data reduction scheme. Issues regarding self-similar crack growth and fracture process zone development are discussed. It was verified that the considered in-plane mix mode fracture criterion is well captured using the proposed data reduction scheme.

KEYWORDS: Bonded joints, fracture characterization, mixed-mode I+II loading, compliance-based beam method.

1. INTRODUCTION

This study uses an apparatus for measuring the toughness of adhesive joints in various fracture modes from mode I (opening) to mode II (shear) relying exclusively on the load-displacement curve obtained from an universal testing machine and the displacement information from two linear variable differential transformer – LVDT - connected to the specimen beams. This apparatus is an evolution from the jig presented by Spelt [1] and its operation is different from those existing on the market, mostly because it does not use the crack length measurement, instead it uses the displacement obtained from the LVDTs. It presents also another great advantage when compared to the existing solutions that places the specimen in the opposite side of the loading jig, because this invention place the specimen inside its structure, thus reducing the overall dimensions and facilitating the required test operations, improving the usability. Relying exclusively on three machine outputs, the load–displacement data and the displacement data from the two LVDTs, shown in Figure 1, it allows an automated data reduction scheme and, therefore, renders an easier analysis that is accurate, not depending on human observation.

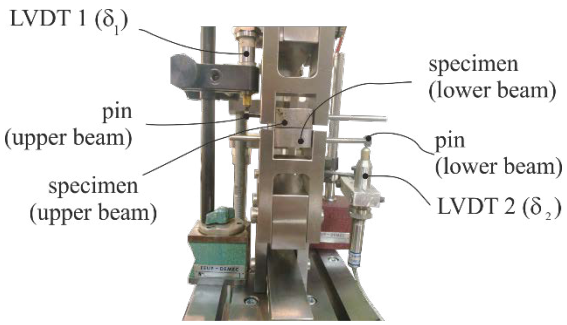

Figure 1.Front view of the Jig, showing the LVDTs.

The loading jig is fully described in Patent number 20131000070010 [2] and is an improvement inspired in the apparatus proposed by Fernlund and Spelt [1] consisting primarily of two rigid beams linked to each other, to the specimen, and to a base plate (Figure 2).

Different jig geometries can be achieved by altering the four distances, s_1 - s_4, thereby varying the mode-mixity of the induced loading. Changing the above referred distances leads to different loads, F_1 and F_2, applied to the upper and lower adherends, respectively, of the tested specimens (Figure 3). Pure mode tests, namely the

* Corresponding author. Tel. +351 22 508 1750
E-mail adress: chaves.filipe@fe.up.pt

DCB for mode I and the ENF for mode II, are also available to perform with this apparatus, proving to be versatile in the context of fracture characterization.

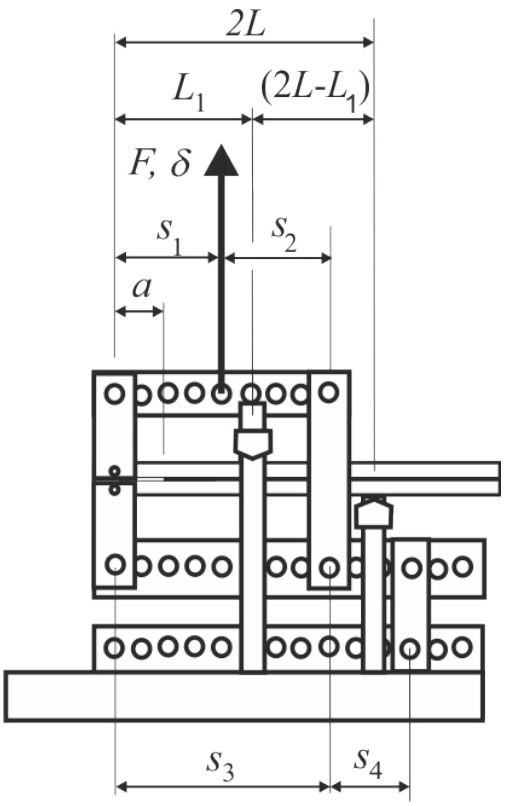

Figure 2. Loading jig schematics.

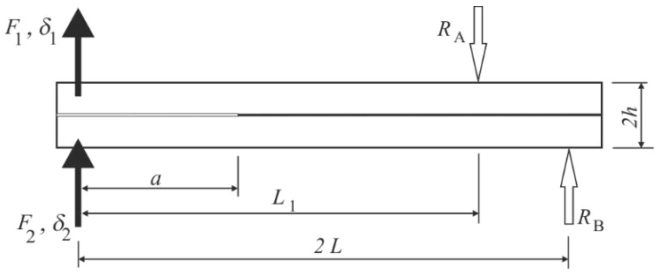

Figure 3. Schematic representation of specimen loading and dimensions (h = 12.7mm, $2L$ = 260mm B = 25 mm is the specimen width).

2. TEST PROCEDURE

The proposed apparatus is fixed into an universal testing machine (UTS) and two linear variable differential transformers (LVDTs) are also set up in place and connected to the UTS data acquisition system. One end of the DCB specimen is connected to the apparatus with two pins that contact with the LVDT measuring rod to measure de displacement of each beam, δ_1 and δ_2. The specimen must be levelled adjusting the back support (wedge beam) that will define the $2L$ dimension (defined in figures 1 and 2) as shown in Figure 4.

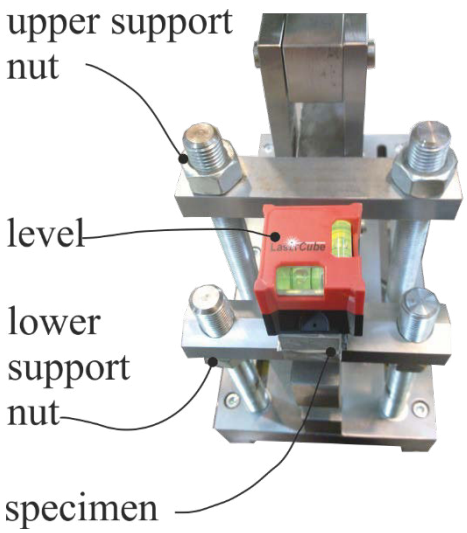

Figure 4.Levelling

3. DATA REDUCTION SCHEME

One important aspect intrinsic to fracture properties measurements is the data reduction method. Usually, the strain energy release rate under mixed-mode (G_T) is obtained by means of the Irwin-Kies equation [3],

$$G_T = \frac{P^2}{2B}\frac{dC}{da} \qquad (1)$$

which requires compliance calibration as a function of crack length. This task is usually cumbersome since crack length monitoring during its propagation can be difficult to perform namely in test where mode II loading predominate, because the crack faces tend to remain in contact during its growth. In order to overcome these limitations an equivalent crack length method was proposed in a previous study [4]. The method uses the current specimen compliance and the Timoshenko beam theory to estimate an equivalent crack length during the course of the fracture test. The second limitation is related to the energy dissipation at the fracture process zone (FPZ) ahead of the crack tip, which can be non-negligible as is the case of adhesives with some inelastic behaviour. The consideration of the

clear crack length (not including the influence of the FPZ size), as a fracture parameter in beam theory equations does not allow accounting for this energy.
To obtain the release rate energies, Chaves at al. proposed:

$$G_{\mathrm{I}} = \frac{6P_{\mathrm{I}}^2}{B^2 h}\left(\frac{2a_{\mathrm{eI}}^2}{h^2 E} + \frac{1}{5G}\right) \quad (2)$$

$$G_{\mathrm{II}} = \frac{9P_{\mathrm{II}}^2 a_{\mathrm{eII}}^2}{4B^2 h^3 E} \quad (3)$$

Equations (2) and (3) provide the attainment of the resistance curves (R-curves), during the test in each mode. The plateau values permit the identification of the strain energy release rate under self-similar crack growth conditions, thus providing the identification of the mode-mixity as well as the total fracture energy of the test. The proposed method only requires the register of the load F by means of the machine load cell and displacement components applied to each arm of the specimen (δ_1, δ_2) during the test, for which two LVDTs were used (Figure 1). The load components (F_1 and F_2) can be easily obtained from the load applied by the machine (F) seen in Figure 5 (left) and static equilibrium of each loading arm (Figure 2).
Figure 5 shows the loading apparatus connected to the universal testing machine and the screens capture for the registered Load (F) and displacements of the upper and lower specimen arms (δ_1, δ_2) on the left and the data reduction scheme diagram on the right.

4. SPECIMENS

The specimen geometry is in accordance with the ASTM D3433-99 [5] manufactured with high grade steel with the DIN code 40 CrMnMo 7. The surface preparation consisted in sandblasting and cleaning with acetone. A pre-crack was made using a razor blade within the spacers used to obtain a constant bondline thickness of 0.2 mm. After adhesive application on the substrates, the joints were cured in a hot press at a constant pressure and temperature. A ductile epoxy adhesive, Araldite® 2015 (Huntsman) was used. This adhesive was already characterized in previous studies [6, 7] for pure modes I and II and a small range of the fracture envelope for mixed-mode I +II.

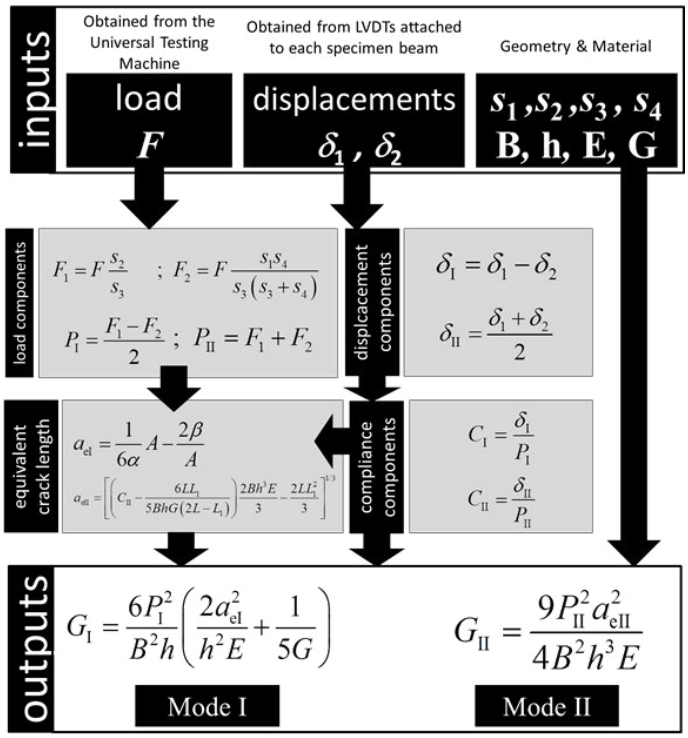

Figure 5. Data reduction scheme.

5. RESULTS

Three combinations for the s_1-s_4 dimensions were tested. Numerical studies [8] indicated that pure mode I (DCB test) was possible to perform, but pure mode II (ENF) could not be achieved. The dimensions to obtain the opening pure mode I were set as s_1=40 mm , s_2 =120 mm, s_3=160 mm and s_4 = -120 mm as shown in Figure 2.
The remaining two combinations, were set in order to obtain a predominant mode I test - s_1=60 mm , s_2 =100 mm, s_3 =160 mm and s_4 = 80 mm - as a second set-up with ψ = 20º and the third set-up to obtain a predominant mode II test with ψ = 85º - s_1 =80 mm , s_2 =60 mm , s_3 =140 mm and s_4 = 100 mm.
The load-displacement (F-δ) curve obtained from the universal testing machine and also the displacements (δ1 and δ2) recorded by the LVDTs at the loading pins, for the first apparatus set up (Figure 2 with s_1=40 mm , s_2 =120 mm , s_3 =160 mm and s_4 = -120 mm) are shown in the graph of Figure 6. Using this data to calculate the energy release rate, it was possible to compute the R-curve for this loading case as shown in Figure 7.

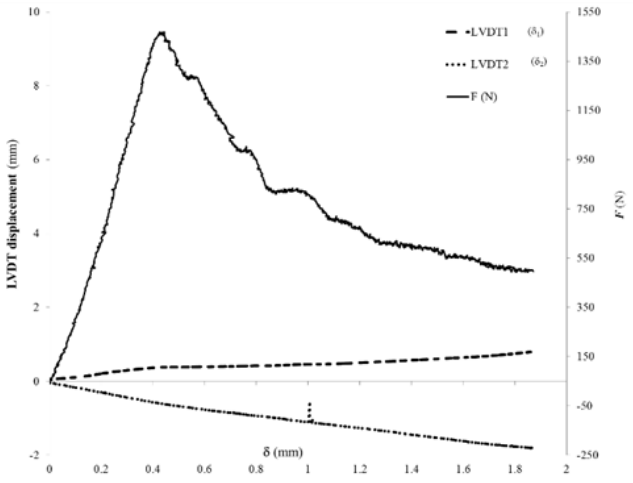

Figure 6. Load displacement and LVDTs displacement curves for pure mode I loading case (s_1=40 mm , s_2 =120 mm , s_3=160 mm and s_4 = -120 mm), ψ = 0º.

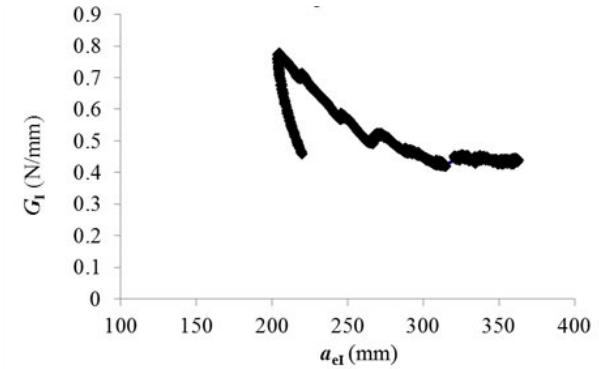

Figure 7. R-curve for the first loading case (pure mode I, s_1 =40 mm , s_2 =120 mm , s_3 =160 mm and s_4 = -120 mm).

The second loading case, (s_1=60 mm, s_2 =100 mm, s_3=160 mm and s_4 = 80 mm) load-displacement (F-δ) and the specimen beams displacements (δ_1 and δ_2) recorded by the LVDTs at the loading pins, are shown in Figure 8. The nominal phase angle of loading ψ for this case is 20º.

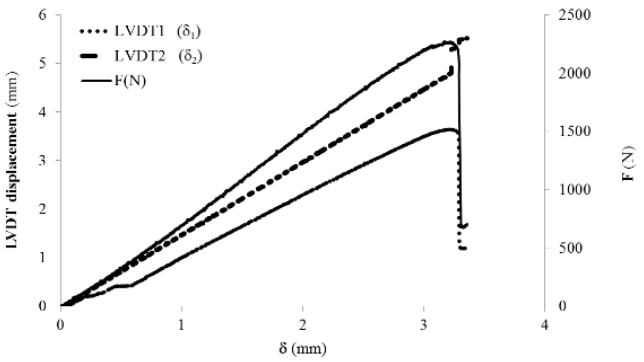

Figure 8.Load displacement and LVDTs displacement curves for the second loading case (s_1 =60 mm , s_2 =100 mm , s_3=160 mm and s_4 = 80 mm), ψ = 20º

The resulting R-curves for mode I and mode II are plotted in Figure 9 and the mode ratio G_I/G_{II} variation is shown in Figure 10.

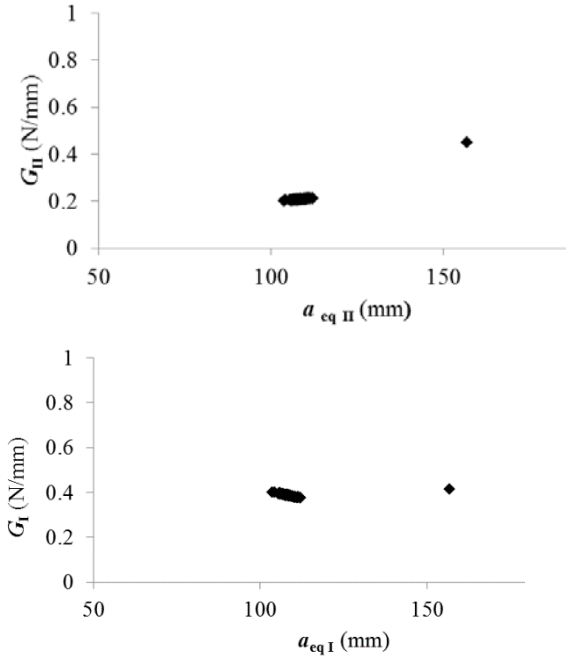

Figure 9. Mode I (top) and mode II (bottom) R-curves for the second loading case (s_1 = 60 mm, s_2 =100 mm, s_3 =160 mm and s_4 = 80 mm).

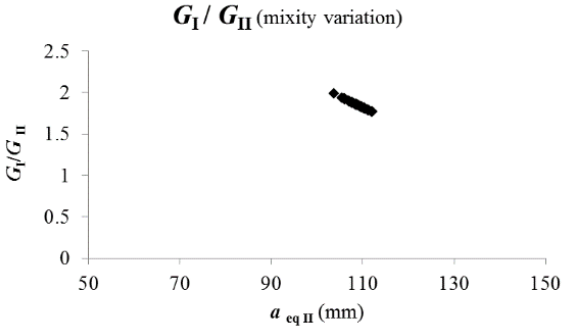

Figure 10. G_I/G_{II} ratio variation for the second loading case (s_1 = 60 mm, s_2 =100 mm, s_3 =160 mm and s_4 = 80 mm).

For the third loading case (s_1=80 mm, s_2 =60mm , s_3=140 mm and s_4= 100 mm), the load-displacement (F-δ) and the displacements (δ_1 and δ_2) recorded by the LVDTs at the loading pins, are shown in . The nominal phase angle of loading ψ for this case is 85º.

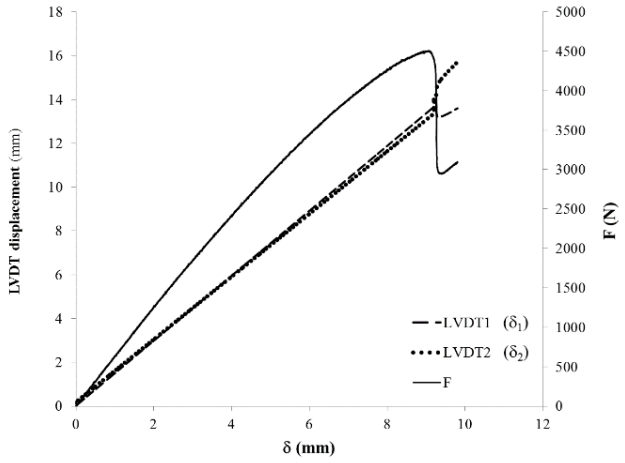

Figure 11. Load displacement and LVDTs displacement curves for the third loading case (s_1=80 mm, s_2 =60 mm, s_3=140 mm and s_4 = 100 mm), ψ = 85º.

Computing this data with the proposed data reduction scheme, the resulting R-curves for mode I and mode II are plotted as shown in Figure 12.

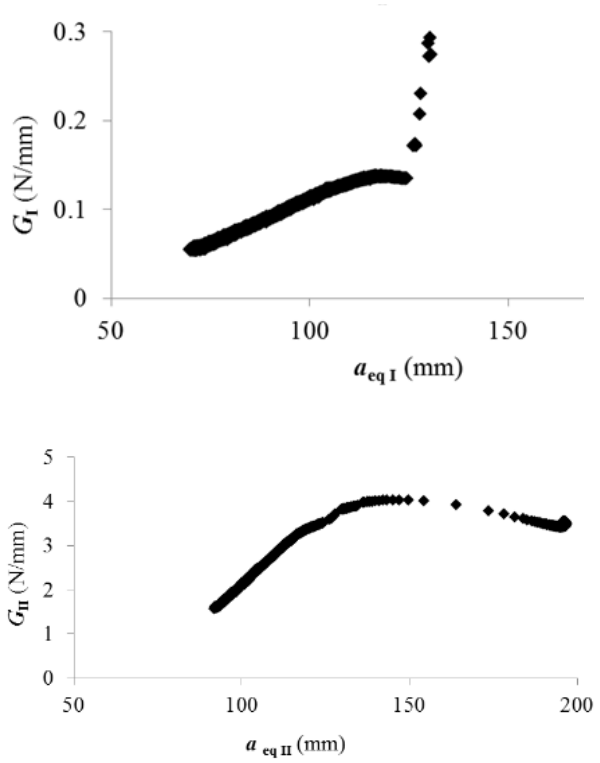

Figure 12. Mode I (top) and mode II (bottom) R-curves for the third loading case (s_1 =80 mm, s_2 =60 mm, s_3 =140 mm and s_4 = 100 mm).

A graph showing the development of the mode-mixity for this test is also plotted in Figure 13.

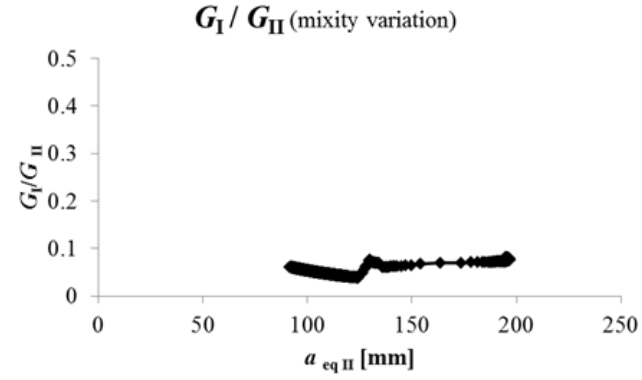

Figure 13. G_I/G_{II} ratio variation for the third loading case (s_1 =80 , s_2 =60 , s_3 =140 and s_4 = 100 (mm)).

Using the previous information, it is possible to obtain a fracture envelop with these three points of the energy release rate in mode I (G_I) and mode II (G_{II}) for each combination as shown in Figure 14.

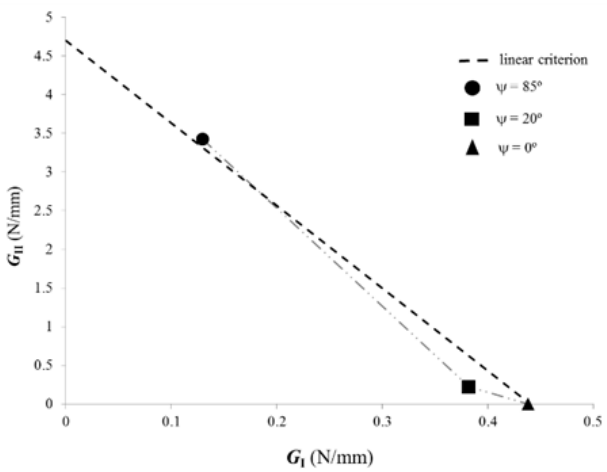

Figure 14. Fracture envelop for the three combinations (ψ = 85º, ψ = 20 º and ψ = 0º).

6. DISCUSSION

The presented apparatus allowed to obtain three different combinations for testing loads in mode I (opening) and mode II (shear) resulting in three different load-displacement curves. Furthermore, each test registered the displacement of the upper and lower specimen beams using a LVDT for each one. The first combination characterized by ψ = 0º, implements a DCB test in pure mode I, and reported a good verification for the ability of this apparatus to perform fracture tests in mode I.

The resulting load-displacement curve (Figure 6) is characteristic of a DCB test, and provides a good approximation to tests previously done by the authors [7] as shown in Figure 15.

The computed energy release rate for this test is plotted in Figure 6 and shows a blunt effect caused by the round tip of the initial crack, and then stabilizes at a plateau near 0.438 N/mm for the mode I energy release rate, G_I. This value is in agreement with previously works published by da Silva et al. [7] and Campilho , Moura et al. [9].

The second combination for a ψ = 20º, provided a mixed mode (I+II) test resulting a load-displacement curve in Figure 9 with a higher value for the maximum force when compared to the first combination. This test results were computed in two energy release rates for both mode I and mode II which are plotted in Figure 9 and shows a plateau near 0.382 N/mm for the mode I energy release rate, G_I , on the left and another plateau near 0.22 N/mm for the mode II energy release rate, G_{II} , on the right. This is in accordance with a mode I predominant test.

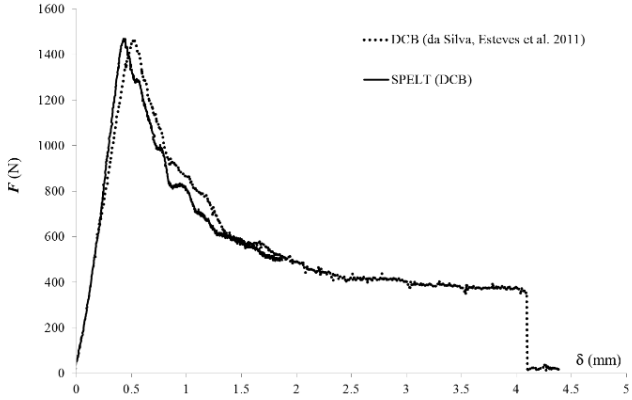

Figure 15. Comparison between the first combination test (DCB, ψ=0º) and a previously performed pure mode I DCB test by da Silva, Esteves et al. (da Silva, Esteves et al. 2011).

The mode mixity ratio G_I/G_{II}, plotted in Figure 10, has little variation showing that this test promotes a self-similar crack propagation.

The third combination with ψ = 85º, provided a mixed mode (I+II) test (Figure 11) with a higher value for the maximum force when compared to the second and first combinations.

Both the load-displacement data and the LVDTs displacements were computed in two energy release rates for both mode I and mode II which are plotted in Figure 12 showing a plateau near 0.13 N/mm for the mode I energy release rate, G_I , on the left and another plateau near 3.42 N/mm for the mode II energy release rate, G_{II} , on the right. The higher value for G_{II} is in accordance with a mode II predominant test as expected. Once again, the mode mixity ratio G_I/G_{II}, plotted in Figure 13, has little variation underlining that this test promotes a self-similar crack propagation.

The values obtained for the energy release rates from the three tests were plotted in a graph in order to obtain a fracture envelop presented in Figure 14.

7. CONCLUSIONS

A test apparatus developed for mixed-mode (I+II) adhesive joint fracture mechanics characterization is presented. Three combinations for different mode

mixities (ψ = 0º, ψ = 20º and ψ = 85º) were tested and the experimental results were analysed with a novel data reduction technique (Chaves, de Moura et al. 2013). The results obtained for the first combination tested (ψ = 0º), proved to be in close agreement with a DCB test performed for pure mode I characterization returning load-displacement values consistent with previous works (da Silva, Esteves et al. 2011) and confirming the same value for mode I toughness (G_I). The second (ψ = 20º) and third (ψ = 85º) combinations tested, allowed to perform a mixity variation that were analysed and gave consistent results within the fracture envelop for Araldite® 2015.

The fracture envelop plotted with the three tests presents a moderately good agreement with the linear criterion. Another interesting point resides in the self-similar crack propagation confirmed by a very low variation of the mode mixity ratios during the performed tests. The test method presented, avoids the crack length measurement that is a time consuming and sometimes impossible task to perform and is also a compact apparatus allowing to test the simplest geometry like a DCB specimen, simplifying the test procedure and specimen manufacture.

This could be a good tool for adhesive joint design, because it allows an easier test, improving the usability and data computation to obtain expedite results.

8. ACKNOWLEDGEMENTS

The authors would like to thank the "Fundação Luso-Americana para o Desenvolvimento" (FLAD) for the support through project 314/06, 2007 and Instituto de Engenharia Mecânica (IDMEC).

9. REFERENCES

[1] Fernlund, G. and J.K. Spelt, Mixed-mode fracture characterization of adhesive joints. Composites Science and Technology, 1994. 50(4): p. 441-449.

[2] Chaves, F.J.P., L.F.M. Da Silva, and M.F.S.F. de Moura, Apparatus and method for characterization of bonded joints mixed-mode I+II fracture, patent number: 20131000070010. 2013, INPI: submitted patent.

[3] Irwin, G.R. and J.A. Kies, Critical Energy Rate Analysis of Fracture Strength. Welding Journal Research Supplement, 1954. 33: p. 193-198.

[4] Chaves, F.J.P., et al., Numerical validation of a crack equivalent method for mixed-mode I+II fracture characterization of bonded joints, Engineering Fracture Mechanics,submitted to JA. 2013: submitted to JA.

[5] ASTM D3433 - 99, Standard Test Method for Fracture Strength in Cleavage of Adhesives in Bonded Metal Joints, in Annual book of ASTM standards. 2012, West Conshohocken, ASTM 15.06. p. 225-231.

[6] da Silva, L.F.M., et al., Mode II Fracture Toughness of a Brittle and a Ductile Adhesive as a Function of the Adhesive Thickness. The Journal of Adhesion, 2010. 86(9): p. 891-905.

[7] da Silva, L.F.M., V.H.C. Esteves, and F.J.P. Chaves, Fracture toughness of a structural adhesive under mixed mode loadings Bruchzähigkeit eines Strukturklebstoffs bei Mixed-Mode Belastung. Materialwissenschaft und Werkstofftechnik, 2011. 42(5): p. 460-470.

[8] Chaves, F.J.P., et al., Numerical validation of a crack equivalent method for mixed-mode I+II fracture characterization of bonded joints. Engineering Fracture Mechanics, 2013. 107: p. 38-47.

[9] Campilho, R.D.S.G., et al., Obtaining the cohesive laws of a trapezoidal mixed-mode damage model using an inverse method. Ciência & Tecnologia dos Materiais, 2008. 20: p. 81-86.